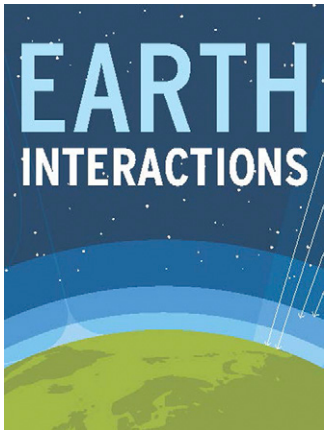

Forest Degradation Associated with Logging Frontier Expansion in the Amazon: The BR-163 Region in Southwestern Pará, Brazil

T. F. Pinheiro[a]

Center for Earth System Science, National Institute for Space Research (INPE), São José dos Campos, Brazil

M. I. S. Escada

Center for Earth System Science, Department of Image Processing, National Institute for Space Research (INPE), São José dos Campos, Brazil

D. M. Valeriano

Amazonia Monitoring Program, Department of Remote Sensing, National Institute for Space Research (INPE), São José dos Campos, Brazil

P. Hostert

Geomatics Lab, and Department of Geography, Humboldt-Universität zu Berlin, Berlin, Germany

F. Gollnow and H. Müller

Department of Geography, Humboldt-Universität zu Berlin, Berlin, Germany

Received 19 February 2015; in final form 24 February 2016

[a] Corresponding author address: T. F. Pinheiro, Departamento de Ciências do Sistema Terrestre, Instituto Nacional de Pesquisas Espaciais, 1758 Av. Astronautas, CEP 12227-010, São José dos Campos, SP Brazil.

E-mail address: taise.pinheiro@inpe.br

DOI: 10.1175/EI-D-15-0016.1

ABSTRACT: Forest degradation is the long-term and gradual reduction of canopy cover due to forest fire and unsustainable logging. A critical consequence of this process is increased atmospheric carbon emissions. Although this issue is gaining attention, forest degradation in the Brazilian Amazon has not yet been properly addressed. The claim here is that this process is not constant throughout Amazonia and varies according to colonization frontiers. Moreover, the accurate characterization of degradation requires lengthy observation periods to track gradual forest changes. The forest degradation process, the associated time-frame, spatial patterns, trajectories, and extent were characterized in the context of the Amazon frontiers of the 1990s using 28 years (1984–2011) of annual Landsat images. Given the large database and the characteristic of logging and burning, this study used data mining techniques and cell approach classification to analyze the spatial patterns and to construct associated trajectories. Multi-temporal analysis indicated that forest degradation in the last two decades has caused as many interannual landscape changes as have clear-cuts. In addition, selective logging, as a major aspect of forest degradation, affected a larger amount of forest land than did forest fire. Although a large proportion of logged forest was deforested in the following years, selective logging did not always precede complete deforestation. Instead, the results indicate that logged forests were abandoned for approximately 4 years before clearance. Throughout the forest degradation process, there were no recurrent forest fires, and loggers did not revisit the forest. Forest degradation mostly occurred as a result of a single selective logging event and was associated with low-intensity forest damage.

KEYWORDS: Geographic location/entity; Amazon region; Observational techniques and algorithms; Data mining; Remote sensing; Applications; Deforestation

1. Introduction

The literature offers several definitions of forest degradation (Lund 2009). However, defining forest degradation can be a challenge because the definition depends on the biophysical conditions, causes, and spatial and temporal scales considered (Sasaki and Putz 2009; Thompson et al. 2013). In addition, the definition should be based on an operational formulation that allows systematic measurements of forest degradation (Simula 2009). In this research, we adopted an operational definition of forest degradation developed by the National Institute for Space Research (INPE; INPE 2008). According to INPE, forest degradation is the gradual and long-term process of canopy-cover reduction because of forest fire or unsustainable logging (INPE 2008).

The contribution of forest degradation to climate change has led to the establishment of an international program that compensates tropical forest countries for reducing their carbon emissions; this program is referred to as Reducing Emissions from Deforestation and Forest Degradation (REDD). Despite the relationship between forest degradation and carbon losses, the substantial amount of greenhouse gases released into the atmosphere as a result of forest degradation has not been appropriately addressed by REDD (Mertz et al. 2012). Furthermore, the dynamics of forest fire and selective logging (SL) activities have not been properly addressed, which has resulted in significant uncertainties regarding carbon emissions (Pan et al. 2011) and has limited the benefits of mitigation actions (Mertz et al. 2012).

These inadequacies have resulted largely from a lack of information regarding forest degradation, which is partly because of the inherent complexity of this process. While rapid deforestation (defined here as forest conversion within 1 year or less) swiftly removes almost all of the forest carbon stock, the carbon losses caused by forest degradation depend on the intensity and persistence of human-induced disturbances (Herold and Skutsch 2011). Forest degradation is therefore difficult to characterize because accurate estimates require lengthy observation periods to track the gradual forest changes caused by fire and/or unsustainable logging (Lambin 1999).

Remote sensing offers many opportunities for monitoring forest degradation, including the extensive coverage of inaccessible areas, such as the Amazon region, and information about historical trajectories in land-cover changes (Herold and Skutsch 2011). Several studies have suggested approaches for detecting selective logging and forest fire using Landsat-type imagery (Asner et al. 2006; Matricardi et al. 2010, 2007; Souza et al. 2005).

Although there are several studies on the use of remote sensing to analyze forest degradation (Matricardi et al. 2010, 2005; Monteiro et al. 2003; Souza et al. 2013, 2003; Wang et al. 2005), this process remains poorly characterized. Specifically, these studies (i) did not focus on the trajectories associated with forest degradation, which are needed to predict areas with high probability of change in land cover (Mertens and Lambin 2000) and to include the historical land-cover changes while estimating carbon fluxes (Ramankutty et al. 2007); (ii) examined only forest degradation that occurred in the Amazon frontiers that opened up in the 1970s, such that their results may not be generalized to the entire Amazon; or (iii) analyzed a set of different regions together, which may hinder understanding of the forest degradation process.

We hypothesize that the socioeconomic, political, and biophysical diversity of the Amazon (Becker 2005) shapes the trajectories, intensity, extent, and timeframes associated with forest degradation. Thus, this process is not likely to be homogeneous throughout the Amazon region, and studies should consider intraregional heterogeneity to adequately examine forest degradation. Taking this heterogeneity into account is important for correctly representing forest degradation in carbon emissions models (Aguiar et al. 2012) or the relative contribution of each emission source (i.e., forest degradation or clear-cut deforestation; Pearson et al. 2014).

Considering the existing knowledge gaps, the focus of the present study is to characterize the forest degradation process (i.e., extent, intensity, trajectories, and timeframe) in the context of the recently opened up deforestation frontier in the Brazilian Amazon. We selected the Novo Progresso County, southwestern Pará, Brazil, as a case study of the frontiers of expansion due to the combination of the high wood stocks, the considerable rate of land-cover dynamics, and the limited information on the forest degradation process in this region.

To perform this analysis, we developed a novel methodology using a long time series of annual Landsat images covering a 28-yr period, landscape metrics, and a data mining technique to define spatial patterns of forest damage intensity. Based on these patterns, we analyzed the main forest degradation trajectories.

In this context, we describe the forest degradation process by addressing the following research questions: (i) What is the extent of forest degradation in the

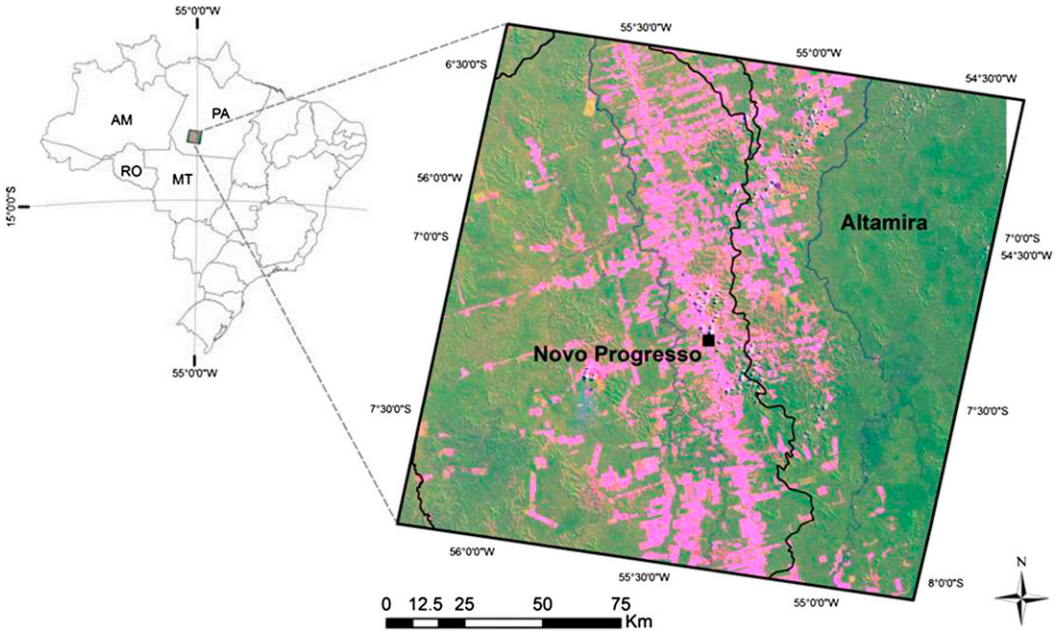

Figure 1. Study site location (Landsat path 227 and row 65) within the Amazon state of Pará (PA), Brazil.

study area? (ii) What is the intensity of forest degradation during the forest degradation process? (iii) What are the main trajectories of forest degradation? (iv) When do the forest degradation trajectories that do not converge to clear-cut begin? (v) Finally, what is the duration of the degradation trajectories in the logging frontiers' expansion?

2. Study area

This study was carried out in Novo Progresso County, southwestern state of Pará, in the Brazilian Amazon (Landsat scene; path 227 and row 65; Figure 1). Novo Progresso County, similar to northwest Mato Grosso State and southeast Amazonas State, is classified as a logging and deforestation frontier with less than 20 years of logging history (Pereira et al. 2010). The natural vegetation consists almost entirely of dense evergreen upland forests; the tallest trees reach 50 m, and the average biomass is 281 Mg ha^{-1} (EMBRAPA 2008; Vieira et al. 2004). Improved transportation infrastructure, such as the paving of the BR-163 highway between Cuiabá and Santarém, allows access to previously inaccessible primary forests. Combined with poor law enforcement, this development has stimulated illegal logging (Fearnside 2005). Official statistics indicate that Novo Progresso is a hotspot of deforestation in the Amazon region, with the fourth highest deforestation rate according to the last estimate (INPE 2013). Approximately 14.25% (5441 km^2) of the forests in this county have been converted to other land-cover types (INPE 2013), primarily cattle production (IBGE 2015; INPE 2010).

Table 1. Landsat imagery (path 227 and row 65) used in this study to map annual forest degradation (1984–2011).

Scene code	Date	Cloud cover (%)
LT52270651984189CUB00	7 Jul 1984	0.01
LT52270651985223CUB00	11 Aug 1985	0
LT52270651986178CUB02	27 Jun 1986	0.01
LT52270651987133CUB00	13 May 1987	0.4
LT52270651988184CUB00	2 Jul 1988	0.05
LT52270651989170CUB00	19 Jun 1989	0.01
LT52270651990221CUB00	9 Aug 1990	6.5
LT52270651991224CUB00	12 Aug 1991	3.5
LT52270651992211CUB02	29 Jul 1992	0.04
LT52270651993213CUB00	1 Aug 1993	0.01
LT52270651994216CUB00	8 Apr 1994	0
LT52270651995187CUB00	7 Jun 1995	0.03
LT52270651996222CUB00	9 Aug 1996	15
LT52270651997176CUB02	25 Jun 1997	0.08
Scene code	Date	Cloud cover (%)
LT52270651998211CUB00	30 Jul 1998	4.51
LT52270651999246CUB01	3 Sep 1999	20
LT52270652000217CUB00	4 Aug 2000	22
LT52270652001283CUB00	10 Oct 2001	2
LE72270652002182PFS00	1 Jul 2002	0
LT52270652003193CUB00	12 Jul 2003	2.1
LT52270652004180CUB00	28 Jun 2004	0.2
LT52270652005198CUB00	17 Jul 2005	0.36
LT52270652006217CUB00	5 Aug 2006	0
LT52270652007172CUB00	21 Jun 2007	0
LT52270652008207CUB00	25 Jul 2008	0
LT52270652009193CUB00	12 Jul 2009	0
LT52270652010212CUB01	31 Jul 2010	0
LT52270652011215CUB00	3 Aug 2011	0

3. Methodology

3.1. Landsat imagery

We used Landsat Thematic Mapper (TM) images (path 227, row 65) from 1984 to 2011 to quantify the extent of forest degradation (Table 1). Radiometrically and terrain-corrected Landsat TM images (level 1T) were acquired from the U.S. Geological Survey (USGS) (http://glovis.usgs.gov/). Images from June to September were selected because of the higher likelihood of acquiring images with low cloud cover during this period (dry season; Câmara et al. 2013).

3.2. Deforestation dataset

We used the existing 30-m resolution deforestation maps from the Amazon Deforestation Monitoring Project (PRODES) for the 2000 to 2013 period (http://www.obt.inpe.br/prodes/) to mask out previously deforested land (exceeding the PRODES minimum mapping unit of 6.25 ha), nonforested land (savannas and grassland), and water surfaces. We created annual deforestation maps for the

period in which PRODES data were not available (1984–99) using the same methodology used in PRODES (Câmara et al. 2013). We used the PRODES forest mask of 2000 to produce deforestation maps from 1984 to 1999 to maintain consistency between the two datasets. Thus, all forest degradation mapping produced in this study was restricted to the PRODES-based forest mask area.

3.3. Mapping annual forest degradation

Landsat TM images (1984–2011) were decomposed into fractions of the three basic components (water/shade, vegetation, and soil) through spectral mixture analysis (SMA), which is available in the Spring 5.1.8 software (Câmara et al. 1996). Three TM bands, that is, the visible red (band 3; 0.63–0.69 μm), the near infrared (band 4; 0.76–0.90 μm), and the shortwave infrared (band 5; 1.55–1.75 μm), were used in this analysis. SMA is widely used to identify fire scars in burned forest (Vasconcelos et al. 2013) as well as log decks, skid trails, and tree-fall gaps, which are key features of selective logging (Monteiro and Souza 2012; Monteiro et al. 2003; Souza et al. 2013, 2005). SMA estimates the abundance of water/shade, bare soil, and photosynthetically active vegetation within each pixel using the spectral signatures of prototypic training areas called endmembers (Shimabukuro and Smith 1991). The endmembers were collected directly from the images using representative pixels of bare soil, green vegetation, and water/shade extracted from unpaved roads, photosynthetically active pastures at peak phenology, and dark water, respectively (Anderson et al. 2005; Souza et al. 2005). The spectral signatures of the endmembers were compared to the typical spectral reflectance curves of these three basic components. This process was repeated for each image.

To enhance the forest degradation signal caused by selective logging and forest fire, we computed a spectral index of forest degradation, referred to as DEGRADI, using the fraction images obtained with SMA [Equation (1)]. This index has been used to improve the detection of forest degradation in the monitoring systems of Amazonia (INPE 2008) and is based on the assumption that the high spectral contrast between soil and vegetation fractions highlights key characteristics of selective logging and forest fires. DEGRADI is defined as follows:

$$\text{DEGRADI} = G \times \frac{\text{Soil}}{\text{GV}} + \text{Off}, \tag{1}$$

where DEGRADI is the forest degradation spectral index, G is the gain, Soil is the soil fraction image, GV is the green vegetation fraction image, and Off is the offset. The gain and offset values were interactively applied to maximize the visibility of features in the image.

Based on the images resulting from the DEGRADI spectral index, a semiautomated technique was applied to map forest degradation on an annual basis. We used features such as skid trails, log decks, and tree-fall gaps as indicators of logged forest and fire scars as indicators of burned forest. The threshold boundaries were adjusted empirically for each date based on the reference values collected from these indicators. Consequently, thematic maps (in the form of polygons) that

represented forest fire and selective logging were obtained. Final visual interpretation was required to distinguish between logged and burned forests because these classes of interest did not form spectrally separable classes in the image. We used the bright strips (usually in conical format) as spectral and spatial indicators of fire scars (Graça 2006; Vasconcelos et al. 2013).

3.4. Field study and accuracy assessment

The forest degradation mapping generated with the semiautomatic technique described above was assessed using ground truth data. We conducted field verification of degraded forests by car and overflight from 1 to 8 August 2014. A 2014 forest degradation map was generated using the same spatial and spectral indicators used to detect forest degradation from 1984 to 2011 (see section 3.3). The 2014 forest degradation map was reserved only for field verification purposes and was not used in the time series analysis. Additionally, we used spatially explicit timber harvesting authorization data [Autorização para Exploração Florestal (AUTEF)] for sustainable forest management projects, provided by the State Environmental Agency (SEMA). The AUTEF information was used for orientation in the field and to collect GPS coordinates of the log landings (clearings in the forest where timber is temporarily stored), log roads, and tree-fall gaps.

The omission and commission errors of the semiautomated technique for mapping forest degradation were estimated through a comparison with the ground truth data (71 samples). The accuracy of forest degradation mapping and the associated kappa statistics were used to describe the mapping results.

3.5. From pattern to process

The aim of this article was to assess forest degradation patterns and their associated processes. Given the large geographic database, we used Geographic Data Mining Analyst (GeoDMA) data mining software, which is able to perform searches of pattern similarity in spatiotemporal data (Korting et al. 2008). The processing steps for pattern classification are described below.

3.5.1. Defining a typology of forest degradation

The first phase of this method is the definition of the spatial pattern typology for the study area. We proposed a typology related to the intensity of forest degradation (Figure 2). Instead of using the polygons themselves, the patterns were represented by regions, that is, a grid of cells that encompass a set of polygons. The gridcell approach allows a description of the landscape structure through landscape metrics. This spatial context is important for characterizing forest degradation because the degradation causes widespread and collateral damage to the surrounding landscape, resulting in distinct spatial mixtures of land-cover classes.

The cell grid is defined by a spatial resolution. To define an appropriate cell resolution, it is necessary to consider the scale of the observed pattern (Saito 2011). We considered the average area of the log decks (380 m^2, min: 120 m^2, max: 750 m^2) and the average distance between them (460 m, min: 230 m, max: 989 m; Pantoja et al. 2011); the typical size of the forest management units (the area of

Spatial patterns	Forest degradation intensity class	Spatial pattern description	Class description	Forest degradation index
	Selective logging: Low forest degradation (LFD1)	Few small and isolated clearings	Manual extraction, highly selective logging (1-5 species removed), indicating no logging planning, roads are constructed to access trees	0.4
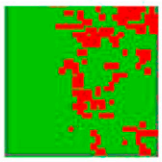	Selective logging: Moderate forest degradation (MFD1)	Intermediate density and size of clearings	Extensive-style logging (5-10 species removed), mechanized, indicating no logging planning; can be cleared or be abandoned	0.5
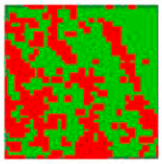	Selective logging: High forest degradation (HFD1)	High density of clearings	Extensive-style logging (>20 species removed), mechanized, indicating no logging planning	0.9
	Conventional logging: Low forest degradation (LFD2)	Small patch of degraded forest	Commercial species can be extracted, but the final objective is a clearcut in the short-term	0.4
	Conventional logging: Moderate forest degradation (MFD2)	Medium patch of degraded forest	Commercial species are extracted, but the final objective is a clearcut in the short-term	0.7
	Conventional logging: High forest degradation (HFD2)	Large patch of degraded forest	Commercial species are extracted, but the final objective is a clearcut in the short-term	0.99
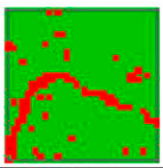	Poor logging practices (PLP)	Small to medium cleared patches associated with linear features	Associated with IFD1 and MFD1 forest degradation patterns. Log roads are created to access species of interest in the forest. Configuration of roads, log landings and clearings reveals harvest planning problems.	0.6

Figure 2. Typology of forest degradation intensity in Novo Progresso, Amazon state of Pará (green color indicates forest and red color indicates forest degradation features, that is, tree-fall gaps, log decks, and skid trails. The HFD2 pattern was very rare in the dataset and represents a fuzzy transition between degraded forest and clear-cut. For this pattern, we arbitrarily attributed a value of 0.99).

allowable harvest per year), which is 1 km^2 (Sabogal et al. 2000); and a cell size of 1 km^2, implemented in previous study to characterize a logged forest (Sato et al. 2011). These previous estimates and findings justify our proposal, that is, the use of a 1-km^2 cell resolution to characterize selective logging areas because the dimensions of all features that characterize this activity are included.

Defining the intensity of forest degradation. Each pattern defined above was associated with a particular intensity of forest degradation. We developed a composite index for the intensity of forest degradation based on the landscape ecology metrics. We used the following metrics: patch area (defined as the internal area of the patches contained within a cell), edge density (the sum of the lengths of all edge segments of a patch type contained within a cell divided by the total area of the patch type), and mean patch size (the sum of the area of a patch type inside a cell divided by the total number of patch types). The landscape ecology metrics were calculated using GeoDMA (see section 3.5.2).

We used the analytic hierarchy process (AHP), a decision support tool available in Spring software (Câmara et al. 1996), to calculate the relative importance of each metric (Saaty 1980). In the AHP test, weights are derived using a set of pairwise comparisons. The user can rate the comparison as equal, marginally strong, strong, very strong, or extremely strong. The final result is assessed through the consistency index (CI values ≤ 0.1 are considered optimal; Saaty 1980). We considered the loss of forest (indicated in the present study by the patch area metric) to be a very strong factor of forest degradation because it can drive populations to direct extinction because of reduced habitat (Uhl et al. 1989). In addition, this factor is correlated with forest fragmentation (indicated in the present study by both the edge density and mean patch size metrics; Tabarelli et al. 2004). We assigned the same importance to the edge density and mean patch size metrics. Although fragment size and forest edge density play important roles in determining the severity of forest fragmentation (Laurance 2004), we considered the forest to degraded forest transition to be less abrupt than the transition between forest and pasture/agricultural areas; as a result, the effects of the forest edge and fragment size on the overall forest structure are expected to be lower. The CI for the pairwise comparisons was estimated as 0.03.

The parameters for the forest degradation intensity are shown in Table 2. The corresponding mean values of landscape ecology metrics were calculated for each pattern. We normalized the mean values by scaling them between 0 and 1. The index for the intensity of forest degradation was calculated as

$$\mathrm{FDI} = (\mathrm{PA}_{\mathrm{norm}} \times W_{\mathrm{PA}}) + (\mathrm{ED}_{\mathrm{norm}} \times W_{\mathrm{ED}}) + (\mathrm{MPS}_{\mathrm{norm}} \times W_{\mathrm{MPS}}), \qquad (2)$$

where $\mathrm{PA}_{\mathrm{norm}}$ is the normalized value for the patch area metric, W_{PA} is the weight for the patch area metric, $\mathrm{ED}_{\mathrm{norm}}$ is the normalized value for the edge density metric, W_{ED} is the weight for the edge density metric, $\mathrm{MPS}_{\mathrm{norm}}$ is the normalized value for the mean patch size metric, and W_{MPS} is the weight for the mean patch size metric.

Forest degradation intensity values closer to 0 indicate low levels of forest degradation, whereas those closer to 1 indicate high levels of forest degradation (0 is considered forest; Figure 2). We further clustered these levels into major categorical classes, defined arbitrarily as low (>0 to ≤ 0.4), moderate (>0.4 to ≤ 0.7), and high (>0.7 to <1), for the forest degradation trajectory analysis.

Table 2. Parameters of the forest degradation intensity index (see Figure 2 for interpreting the acronyms).

Indicator of forest degradation	Landscape metric	Weight	Spatial pattern	Mean value	Normalized value
Forest loss	Patch area	0.714	IFD1	2.2	0.40
			IFD2	3.2	0.36
			MDF1	7.7	0.44
			MDF2	13.9	0.72
			PLP	6.8	0.64
			HDF1	29.4	0.90
Forest edge	Edge density	0.143	IFD1	22.9	0.39
			IFD2	15.5	0.60
			MDF1	68.0	0.49
			MDF2	95.2	0.80
			PLP	47.2	0.64
			HDF1	179.1	0.89
Forest size	Mean patch size	0.143	IFD1	0.14	0.46
			IFD2	1.16	0.26
			MDF1	0.23	0.74
			MDF2	0.45	0.41
			PLP	0.41	0.57
			HDF1	0.68	0.58

3.5.2. Classification of the patterns of forest degradation

To classify the forest degradation patterns, we calculated the landscape ecology metrics for each grid cell. We then constructed a training set for the forest degradation patterns by selecting representative cells for each previous user-defined typology. In the classification step, this training set was used to run a decision tree classifier based on the C4.5 algorithm (Quinlan 1993).

We used 113 samples of forest degradation patterns to train the decision tree classifier [FOREST = 32; selective logging, high forest degradation (HFD1) = 7; conventional logging, high forest degradation (HFD2) = 13; selective logging, low forest degradation (LFD1) = 21; conventional logging, low forest degradation (LFD2) = 13; selective logging, moderate forest degradation (MFD1) = 12; conventional logging, modest forest degradation (MFD2) = 8, and poor logging practices (PLP) = 7]. The samples were acquired from different years. The C4.5 algorithm automatically generated a decision tree with three metrics and four levels (Figure 3). The decision tree used the patch area metric (defined by the internal area of the landscape objects contained within a cell) to distinguish smaller objects from larger ones, the mean patch size metric (defined by the sum of the area of the objects inside a cell divided by the total number of objects) to distinguish cells with a distinct number of patches, and the edge density metric to distinguish cells with different degrees of edges of the patches contained within them.

The accuracy of the forest degradation pattern classification was evaluated by a second expert interpreter. We randomly selected from the automatic classification approximately 50 cell samples of each pattern (the number of cells varies with the representation of each pattern in the dataset), which were interpreted by the second

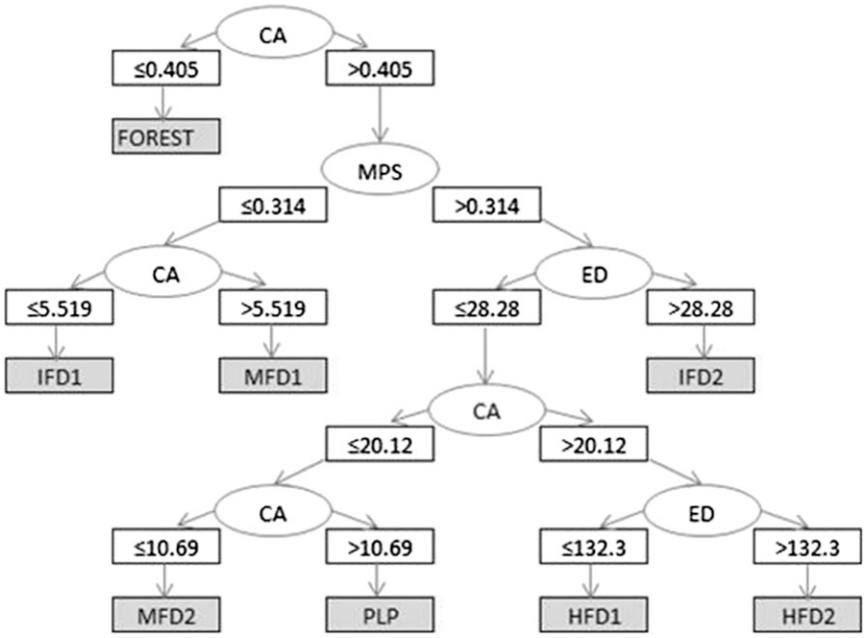

Figure 3. Decision tree for the forest degradation spatial patterns. The landscape metrics are area (CA), edge density (ED), and mean patch size (MPS; for other acronyms; see Figure 2).

interpreter according to the typology presented in Figure 2. We then compared both classifications, computed the confusion matrix, and derived the overall accuracy, the omission and commission errors, and the kappa statistics (Table 3; Congalton and Green 1999; Hudson and Ramm 1987). Confusion matrices, which are often used to describe the performance of a classification, express the number of samples assigned to a particular category in one classification relative to the number of samples assigned to a particular category in another classification (Congalton and Green 1999). The confusion matrix shows the results of interpreter one in columns and the results of interpreter two in rows (Table 3). The overall accuracy between the two classifications, that is, the correctly classified samples indicated by the major diagonal and divided by the total number of samples in the entire confusion matrix, was estimated at 82%. Most of the error, revealed in the confusion matrix, is associated with the misclassification of PLP as MFD1, MFD2, LFD1, or LFD2. These misclassifications are likely because (i) PLP is associated with the logging infrastructures, which can cause extensive degradation similar to the spatial pattern found in LFD2 and MFD2; and (ii) PLP also includes the spatial characteristics observed in IFD1 and MDF1, such as logging roads created to access the tree species in the forest.

The accuracy of the confusion matrix was expressed by the kappa coefficient and was estimated as 79%. The kappa coefficient is a measure of how well two classifications agree with each other; values greater than 0.61 are considered substantial (Landis and Koch 1977).

Table 3. Confusion matrix of the classification of forest degradation patterns (see Figure 2 for interpreting the acronyms). The main diagonal, presented as boldface in the matrix, shows the cases correctly allocated.

		Interpreter 1 (reference)									
	CLASS	PLP	MFD2	MFD1	LFD2	LFD1	HFD2	HFD1	FOREST	Total	Commission error (%)
Interpreter 2	PLP	**34**	4	4	6	2	0	0	0	50	32
	MFD2	6	**34**	0	0	0	3	1	0	44	22.7
	MFD1	1	9	**41**	0	0	2	0	0	53	22.6
	LFD2	8	1	2	**40**	1	0	0	0	52	23.1
	LFD1	1	0	2	3	**47**	0	0	0	53	11.3
	HFD2	0	0	0	0	0	**38**	10	0	48	20.8
	HFD1	0	2	0	0	0	4	**35**	0	41	9.8
	Forest	0	0	0	0	0	0	0	**50**	50	0
	Total	50	50	49	49	50	47	46	50	391	
	Omission error (%)	32	32	16.3	18.4	6.0	19.1	23.9	0		
Overall accuracy = 82%				Kappa coefficient = 79%							

3.6. Analysis of the land-cover change trajectories

We used cells to group the successive transitions between land-cover patterns (i.e., forest, distinct patterns of forest degradation, and clear-cutting intensity) into different land-cover trajectories for the period from 1984 to 2011. All possible trajectories were reduced to the four major trajectories shown in Table 4. Expressions such as "forest degradation persistence," "forest persistence," or "not converted" only have meaning relative to the temporal sample of observation. We calculated the timeframe of forest degradation by calculating the time between the detection of the initial human disturbance and the forest clear-cut. During this process, site abandonment was defined as logged and burned forests that recovered sufficiently such that they were undetectable for one or more years prior to the following human-induced disturbance. The abandonment time was calculated as the time between the forest recovery and the second harvest cycle or fire event. Full forest recovery was assumed if the degradation levels returned to a stable forest status.

4. Results and discussion

4.1. Accuracy of forest degradation detection

We mapped 10 800 km^2 of logged forest, and 8 km^2 of forest degraded because of forest fire during the 28-yr observation period. The results clearly show that selective logging is the most important factor contributing to forest degradation in the study area. This finding is in agreement with previous studies that demonstrate that selective logging has affected a larger amount of forest than has forest fire (Matricardi et al. 2010). As fire scars may became undetectable within 1 year (Matricardi et al. 2010), the annual observation method applied here could result in underestimates of the extent of forest fire in the study area. Furthermore, Landsat satellite images have technical limitations in detecting scars of low-intensity forest fire (Vasconcelos et al. 2013); therefore, it is likely that the degraded forest derived from those areas was not fully captured in this study. However, field observations

Table 4. Interpretation of four, main, land-cover trajectories analyzed for the period from 1984 to 2011 (1 is forest persistence, 2 is forest degradation persistence, 3 is forest degradation cleared, 4 is cleared, and t is time).

	Land-cover sequences			
	t1	t2	t3	Description
1	Forest	Forest	Forest	Pristine forest that remain unchanged since 1984.
2	Forest	Forest degradation	Forest degradation	Forest is not converted into a clear-cut after selective logging/forest fire; indicates forest degradation is ongoing.
3	Forest	Forest degradation	Clear-cut	Single or repeated events of selective logging/forest fire, culminating in forest conversion into a clear-cut.
4	Forest	Clear-cut	Clear-cut	Forest conversion into a clear-cut in a timeframe of one year or less. No selective logging/forest fire events are detected.

support our findings that fire in the study area is typically associated with the conversion of forest/logged forest into clear-cut. This is a plausible view considering that fire is commonly used in forest conversion throughout the Amazon region (Morton et al. 2008) and that heavily burned forest drastically changes the forest structure (Barlow and Peres 2008; Cochrane and Schulze 1999), which can easily lead to forest conversion (Cochrane 2003). Once an area is converted into a clear-cut by fire, it is detected and included in the deforestation map of PRODES. As a result, such areas were no longer subject to analysis in this study. Consequently, PRODES may have mapped the largest amount of area resulting from heavily burned forest in the study area. However, the extent of low-intensity fire needs to be better understood in the new logging frontiers.

The accuracy assessment was performed by comparing binary mapping, forest and logged forest, derived from Landsat images (in rows) and 71 ground truth points (reference data in columns; Table 5). The omission error was dominated by the misclassification of selective logging as forest (omission error = 11%). This error occurred inside the sustainable forest management areas and was associated with collateral damage caused to trees during logging operations, for example, tree felling and the construction of log landings and logging roads. It is estimated that for every tree that is logged, 20 others are damaged, even in planned logging operations (Johns et al. 1996). However, trees usually experience low levels of damage (Johns et al. 1996), which can be observed in the field but are not visible in Landsat images. Similar observations have been reported in previous studies (Matricardi et al. 2007). The log landings, log skidding paths, and large tree-fall gaps effectively facilitated the detection of selective logging, as shown in previous studies (Matricardi et al. 2005; Monteiro et al. 2003). Using these logging features during the visual interpretation processes of our detection approach (see section 3.3), the detection of logged forest was very precise, with no commission errors.

4.2. Analysis of the patterns of forest degradation

We chose three time periods to characterize the temporal distribution of the forest degradation patterns (Figure 4). These three periods represent key moments

Table 5. Accuracy assessment of forest degradation mapping.

Classified data	Reference data		Total	Overall kappa statistics	Overall mapping accuracy
	Logged forest	Forest			
Logged forest	41	0	41	0, 8	0, 9
Forest	5	11	16		
Total	46	11	57		
Omission error	0	31			
Commission error	10, 8	0			
Kappa statistics	1	0, 61			

in land-cover changes, reflecting different migration periods (1984–97) and major changes in the political and socioeconomic framework (2005–11). The largest changes in forest land occurred in the 1998/97 period, mainly because of forest degradation (Figure 4). Part of the degraded forest recovered in the following period (2005–11), and 70% of the original forest land in 1984 was observed in 2011.

In each of our analysis periods, forest degradation was dominated by highly selective logging that is associated with the harvesting of as few as one or two species (LFD1; Figure 5). Although the region has become an important logging center, the high transportation costs have limited the number of tree species harvested, and only the more economically valuable tree species are profitable. This pattern has been observed in other little developed logging regions (Veríssimo et al. 2008). Consequently, we observed that the patterns associated with the moderate to extensive style logging (MFD1) and the extensive style logging (HFD1) remain poorly expressed in the study area. However, the paving of the BR-163 highway between Cuiabá and Santarém will decrease transportation costs and might increase the economic viability of harvesting a greater number of tree species.

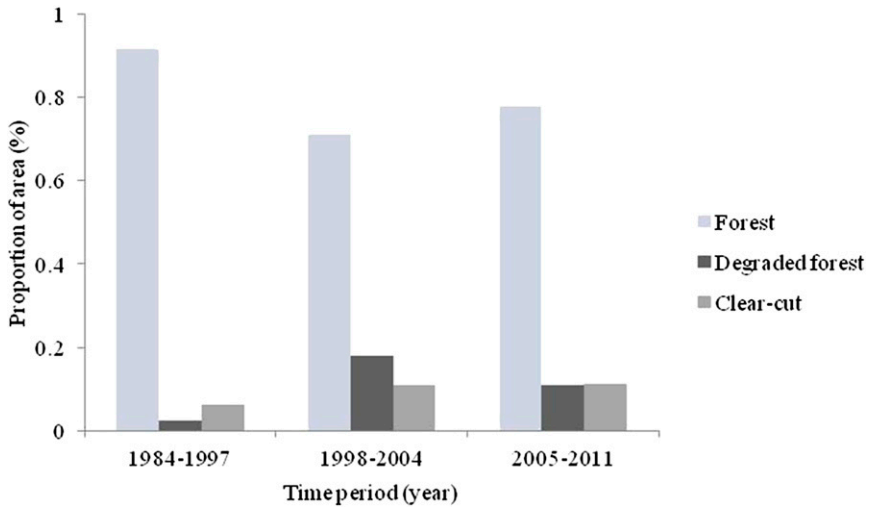

Figure 4. Proportion of degraded forest and clear-cut relative to intact forest in the context of each time period.

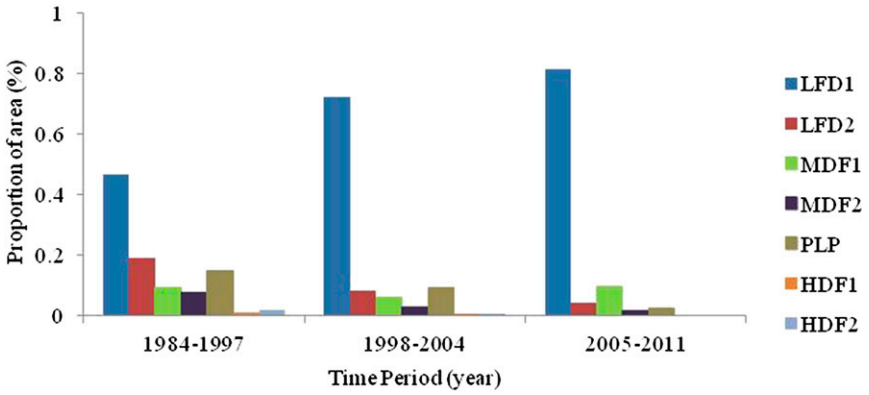

Figure 5. Proportion of area represented by the forest degradation patterns in each period: LFD1, LFD2, MFD1, MFD2, PLP, HDF1, and HDF2.

In the earlier part of the observation period (1984–97), the LFD1 pattern was observed as a result of the migration of settlers and gold miners to the region and their use of wood to develop local infrastructure (Oravec 1998). Then, from the late 1990s, a second migration cycle occurred that was influenced by the paving project of the BR-163 highway; the subsequent demand for wood increased the occurrence of the LFD1 pattern. It was expected that the same trends would be observed for the PLP pattern that was associated with logging infrastructure to access the trees. However, we observed that the occurrence of this pattern decreased along the time series. It appears that the logging practices associated with the planned operations increased in Novo Progresso (SEMA 2015), whereas the region faced increasingly restrictive regulations after 2004 and, consequently, the occurrence of poor logging practices decreased from the first to the last period of observation. However, selective logging activity remains largely illegal in Novo Progresso.

Similar to the earlier period (1984–97), vegetation in the period 1998–2004 was mainly characterized by a low intensity of forest degradation (LFD1 and LFD2), but moderate (MFD2 and MFD1) and high (HFD1 and HFD2) intensities of forest degradation showed unprecedented increases in the region.

4.3. Analysis of the land-cover change trajectories

We observed that 43% of the forest land in the study area changed throughout the 28-yr observation period (1984–2011). Approximately 47% of these land-cover changes were due to rapid deforestation, that is, the replacement of forest by clear-cuts in the timeframe of 1 year or less, referred to here as the cleared trajectory, and 50% of these changes were due to the forest degradation process (degradation/persistence and degradation/cleared trajectories; there was 3% deforestation prior to 1984). Of these degraded areas, 19% were cleared (degradation/cleared trajectory) and 31% remain as degraded (degradation/persistence trajectory).

The 28-yr time series analysis showed that the land-cover dynamic was not uniform over time; instead, the preferential trajectory for which land cover changed

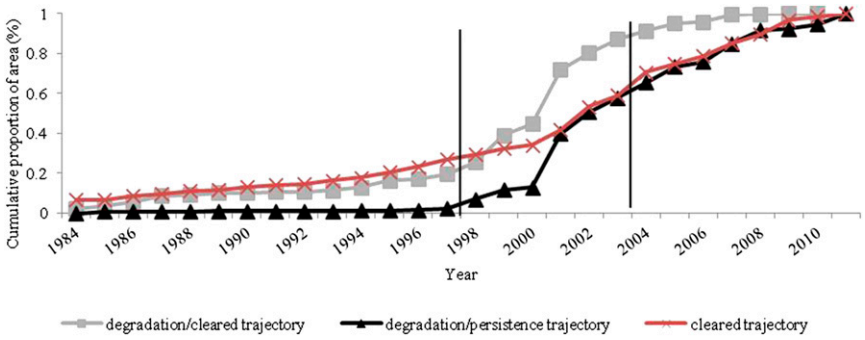

Figure 6. Land-cover change trajectories: evolution from 1984 to 2011.

differed between the periods (Figure 6). Prior to the late 1990s (1984–97), the extent of the overall changes was low (14% of observed land-cover changes), but approximately 80% of the changes were attributed to rapid deforestation (cleared trajectory; Figure 7a). At that time, the timber industry was not yet established, and timber was primarily used locally (Oravec 1998). Deforestation was mainly caused by artisanal gold mining (*garimpo*) and government-sponsored colonization projects (Castro et al. 2004). Although the extent of the overall changes was low, the forest areas had a high probability of being cleared. We observed that approximately 90% of the degraded forests in the period 1984–97 were converted into clear-cut deforestation within 1 year (Figure 7a).

Our results showed that the extent of the land-cover changes increased from the late 1990s when a new migration cycle occurred in anticipation of the BR-163 highway paving project (Ros-Tonen 2011; see Figure 4). Since the 2000s, the timber sector has experienced a sixfold increase in the number of sawmills operating in this region (Carvalho et al. 2002). As a consequence, forest degradation became increasingly more important in contributing to forest changes, and since 1998, according to Figure 6, the forest degradation is the main trajectory for which land cover has changed. Notable increases in the overall extent of degraded forest were observed, increasing progressively from less than 4 km^2 in 1990 to 552 km^2 in 1999 and reaching 1838 km^2 in 2001.

From the late 1990s to the mid-2000s (1998–2004), a 53% change in land cover was observed in the study area. Approximately 40% of these changes occurred as a result of rapid deforestation (cleared trajectory), and 60% were due to forest degradation, indicating a different temporal dynamic compared with the earlier period (Figure 7b). Although 40% of the forests degraded in the period 1998–2004 were converted in 1 year, there was a high percentage of degraded forest (approximately 40%) that was not converted into clear-cut (see Figure 7b, indicated by the value > 28). This result indicates that although the extent of clear-cut deforestation increased relative to the earlier period (1984–97), there was a trend toward the abandonment of degraded forest.

During the period 2005–11, forest degradation and clear-cutting rates began to decline, although not to the level observed prior to 2001, showing 33% of the overall land-cover changes detected in the study area (see Figure 6). The overall reduction in

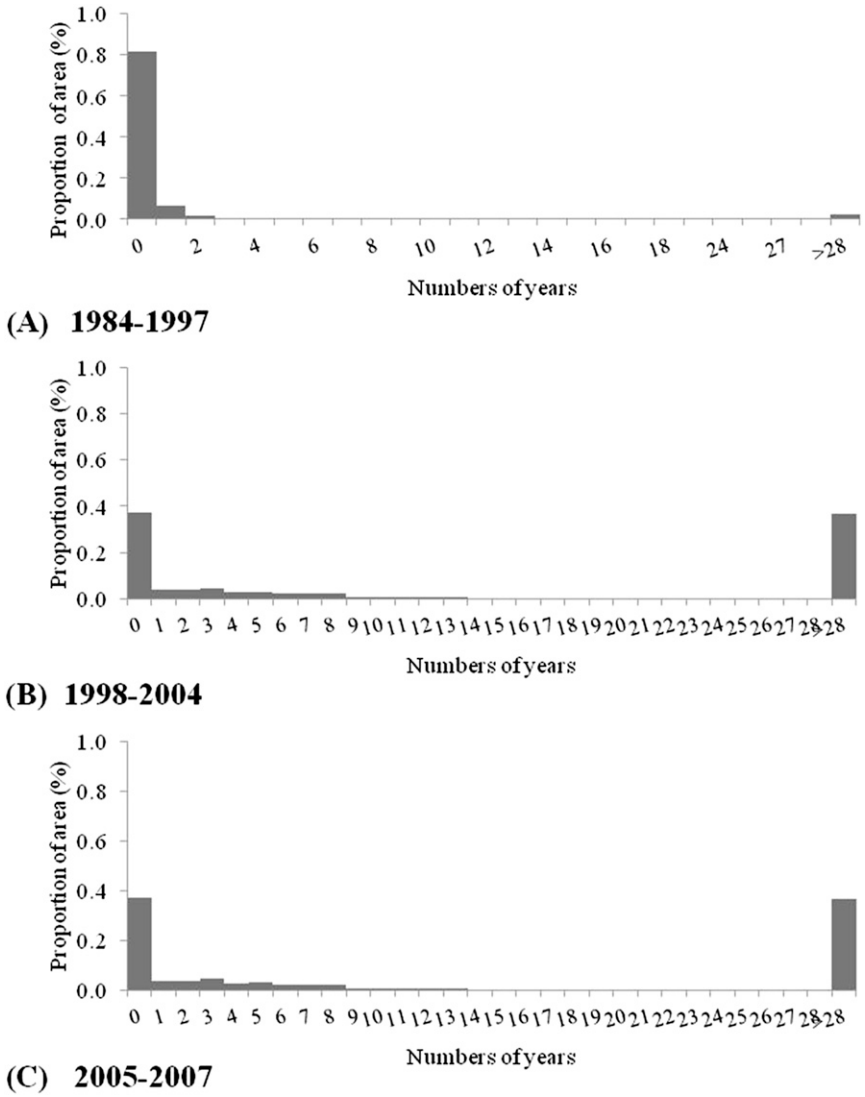

Figure 7. The fate of the degraded forest in each period (*x* axis: the value 0 represents the cleared trajectory, the value 1 to 28 represents the forest degradation-cleared trajectory, different years mean the number of years until deforestation after detection of initial degradation, and the value > 28 represents the forest degradation persistence trajectory).

the extent of the land-cover changes was partly associated with the increasingly restrictive regulations in the Amazon region, including the launch of the Plan for the Protection and Control of Deforestation in the Amazon (PPCDAM; Valeriano et al. 2012), the implementation of a traceability system for timber [Document of Forestry Source (DOF)], and the Environmental Crimes Law, which specifies jail sentences for illegal burning and unsustainable logging (Nepstad et al. 2002).

During the period 2005–11, our results indicated similar proportion between rapid deforestation and deforestation resulting from forest degradation, that is, 55%

of the changes occurred through rapid deforestation (cleared trajectory), and 45% were due to forest degradation. However, we continued to observe a trend toward site abandonment after selective logging. Approximately 40% of the degraded forests in the period 2005–11 were not converted into clear-cut until 2011 (Figure 7c). This might be partly due to the effect of the end of the observation period. However, considering that approximately 50% of the degradation-cleared trajectory was converted in 3 years (see next section), we would expect to observe a low proportion of degraded forest from 2005 to 2011 that was subsequently abandoned after initial degradation. We therefore attributed the high proportion of the abandonment of degraded forest to the advancement of forest management plans and surveillance operations.

The analysis of the percentage of the total area affected by each land-cover change trajectory revealed that 87% of the unchanged forest (i.e., forest persistence) in the study area is inside of protected areas and sustainable human settlements (Figure 8). However, we detected a considerable number of cleared and degradation/cleared trajectory cells within the Jamanxim National Forest, even after its creation in 2006. In contrast, the Bau Indigenous Land contains a large percentage of unchanged forest (97% of its area), partly due to the downsizing of its territory by 317 000 ha in 2003 (Federal Law No. 1.487/2003) after conflicts with farmers and loggers who invaded this indigenous land (see the resized portion in Figure 8).

The land-cover trajectory within the sustainable human settlements that were created in the 2000s by National Institute for Colonization and Agrarian Reform (INCRA) is typically characterized by the forest/persistence (43%) and degradation/persistence (23%) trajectories (Table 6). In contrast, the human settlements that were created in the 1990s are typically characterized by the cleared (34%) and degradation/cleared trajectories (39%; Table 6). Unlike the human settlements, the sustainable human settlements are associated with economic activity based on the sustainable use of forest resources.

In summary, the results show two distinctive processes that lead to the clearing of a forest. First, the extraction of high-value species that causes gradual changes in canopy cover but does not necessarily lead to clearing of the forest, especially if the sustainable use of forest resources is implemented. Second, land conversion associated with clear-cutting for human settlements, land speculation, and agriculture, which occurs immediately after logging. In general, there is an expansion of this second process moving outward from towns and roads.

4.4. The process of deforestation in an Amazon frontier of logging expansion

Forest degradation that led to the clearing of the forest (referred to here as the degradation/cleared trajectory) was mostly characterized by a single selective logging event associated with low to moderate forest degradation. As discussed above, periodic forest fire events were not detected. The main land-cover changes throughout this process are shown in Figure 9. Although multiple selective logging events were detected throughout the forest degradation process, in most cases, previously logged forests were not revisited by loggers for a new harvest cycle. Instead, temporary or

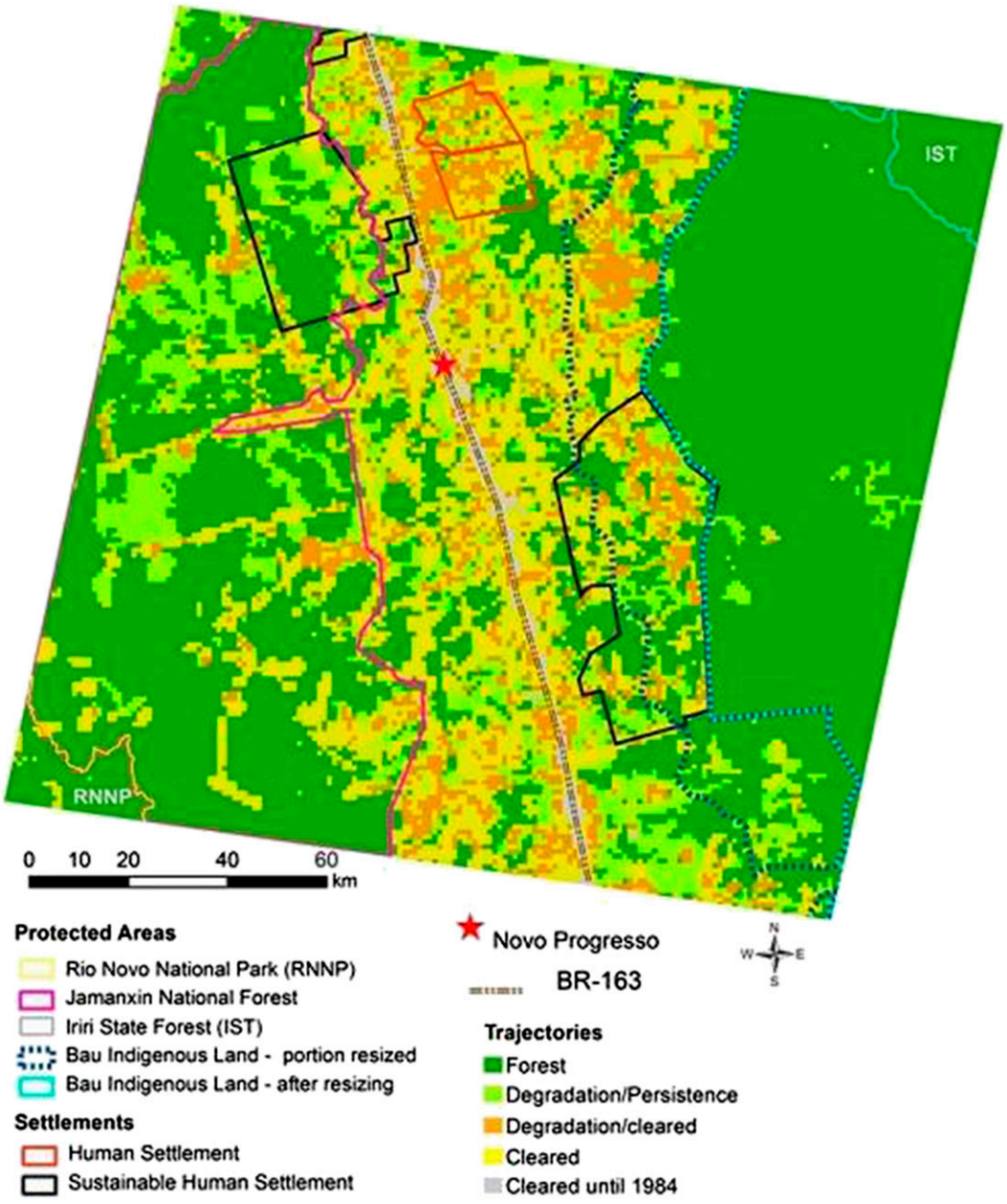

Figure 8. The land-cover cell trajectories surrounding the town of Novo Progresso, an Amazon frontier of logging expansion, illustrating the deforestation process along the BR-163 highway and according to land designation (protected areas and settlements).

permanent site abandonment is the dominant process after selective logging events accounting for 80% of all logging trajectories in this study area.

The forest degradation process in the study area usually began with patterns associated with low and moderate forest degradation intensity (Figure 9).

Table 6. Percentage of the total area of settlements and protected areas affected by each land-cover change trajectory (values in parentheses represent the area in km^2).

Trajectory	Sustainable human settlements	Human settlements	Jamanxim National Forest	Bau Indigenous Land	Iriri State Forest	Rio Novo National Park
			Coverage % — (km^2)			
Cleared	22 (581)	34 (167)	13 (1154)	0	0	7
Degradation/cleared	12 (318)	39 (189)	4 (323)	0	0	0
Degradation/persistence	23 (606)	15 (72)	16 (1441)	3 (153)	0	(1)
Forest/persistence	43 (1143)	12 (59)	67 (5933)	97 (5906)	100 (492)	93 (395)
Deforestation until 1984	0	0	0	0	0	0
Total area (km^2)	2661	487	8852	6098	492	427

Approximately 80% of the initial degradation was associated with the IFD1 pattern, which is associated with the harvesting of a small timber volume from the forest, particularly profitable species (Veríssimo et al. 2008). Extensive style logging (MFD1) and PLP patterns were also detected in the first year, and each accounted for 10% of the logging activity. The few sequences with more than one SL event also indicated a predominance of low forest degradation intensity. Site abandonment contributed to these trends (i.e., toward the predominance of low-intensity patterns) by permitting the recovery of forest biomass. These forest canopies impacted by SL activities are able to recover rapidly after abandonment and can regenerate within 1 to 3 years (Matricardi et al. 2005).

We found that 50% of the logged forest was subsequently deforested within 3 years, 70% was deforested within 4 years, and 90% was deforested within 8 years (Figure 10). A very low proportion of logged forest was deforested after 8 years. Previous assessments have noted distinct trends with respect to the number of years between logging and forest conversion. For example, Asner et al. (2006) found that 36% of a logged forest in Pará State was deforested after 4 years. This result might partly reflect the particular history of the study site because the study conducted by Asner et al. (2006) encompassed regions that varied in agrarian structure, population density, urbanization level, protection status, percentage of original forest, and timber stocks.

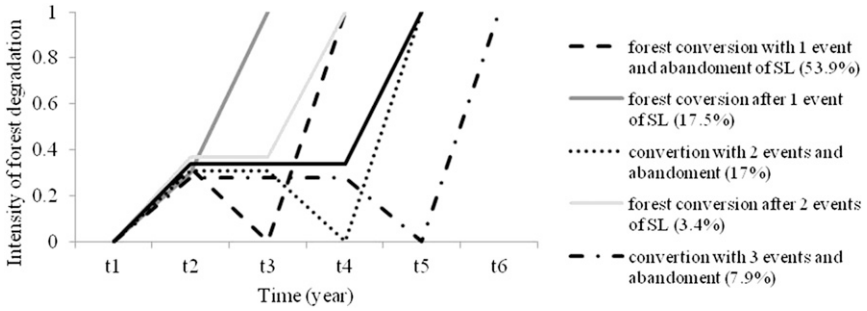

Figure 9. Main trajectories associated to the forest degradation process (SL: selective logging).

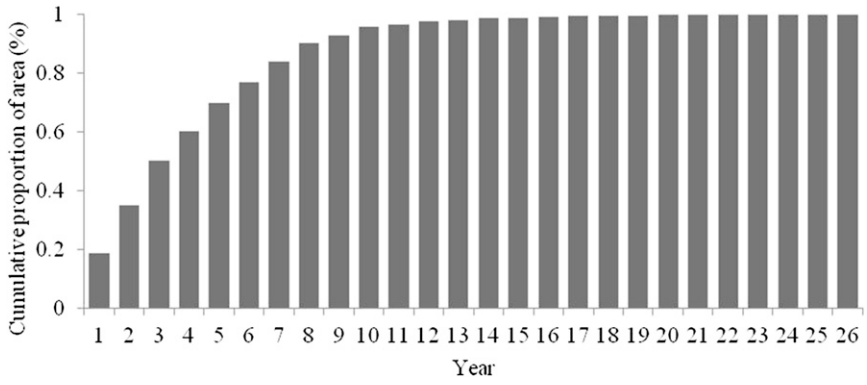

Figure 10. Numbers of years between detection of initial degradation and forest conversion into clear-cut.

5. Conclusions and final remarks

Although studies have shown that degradation in tropical forests occurs over large areas, there is limited knowledge of this process with respect to selective logging, forest fire, and abandonment dynamics. In this study, we characterized the forest degradation process of a frontier expansion based on a long time series of Landsat imagery. However, transferability of our findings on the degradation process to other regions needs to acknowledge the specific geographic settings, for example, the colonization history, protection status, and timber stocks.

During the research period, we found that selective logging was the most important agent of forest degradation. Timber harvesting progressively increased in the study area and was responsible for damaging a larger area of the forests than was clear-cutting after the year 2000. We mapped 10 800 km^2 of logged forest and 8880 km^2 of clear-cut deforestation during the 28-yr observation period. These findings agree with previous studies that demonstrated that the forest has been increasingly affected by selective logging activities (Matricardi et al. 2010, 2013, 2005).

During the forest degradation process, selective logging was mostly associated with patterns of low-intensity forest damage. The role of fire in promoting landscape changes was mostly related to the conversion of forest into clear-cuts, and a regime of recurrent forest fires was not detected in the region.

However, in contrast to previous results (Asner et al. 2006; Matricardi et al. 2013), the forests were not revisited several times by loggers to harvest additional tree species. Instead, we detected only one harvest cycle followed by abandonment. We found that degradation trajectories that converge to clear-cut typically take approximately 4 years (70% of the degradation/cleared trajectory) in the new occupation frontier areas in Amazonia. These results must be considered conservative because the nonvisible forest degradation usually associated with low levels of selective logging and low-intensity forest fire cannot be properly detected on Landsat satellite images (Matricardi et al. 2013; Souza et al. 2003; Stone and Lefebvre 1998). Furthermore, Matricardi et al. (2005) observed that evidence of

logging activities can disappear within 1 year. Thus, yearly observations can underestimate the onset of degradation.

During the observed period (1984–2011), the forest degradation trajectories did not generally result in clear-cuts. Rather, we observed that selective logging activity is often abandoned, allowing forest recovery. This type of degradation trajectory, which does not converge to clear-cut, typically began in the early 2000s, specifically after 1998, when the timber sector increasingly grew in the region.

Implications for carbon emissions from forest degradation

The magnitude of each land-cover trajectory described here has distinct implications for carbon emissions. We showed that before the year of 1998, the trajectories of forest degradation were rare, and the cleared trajectory was the main pathway for which land cover is changed. This finding suggests setting the baseline for carbon emissions due to forest degradation in the region at the end of 1990s (i.e., 1998), when the forest degradation progressively increased in Novo Progresso. However, the baseline for the Amazon frontiers that opened up in the 1970s still requires analysis, since their long-lasting land-use history as well as socioeconomic, political, and physical differences might result in a different land-cover dynamic.

Knowledge of the relative contribution of each carbon emission source is important for designing appropriate surveillance actions and to correctly represent carbon emissions in models. The contribution of forest degradation to overall carbon emissions depend on the timeframe of the process, the intensity of degradation, the fate of the timber, whether the process results in clearing, and the extent of forest degradation. Because these aspects can change over time, the forest degradation process in the distinct Amazon frontiers should be characterized and differentiated, providing a better understanding of the role of forest degradation trajectories in carbon emissions.

Acknowledgments. The author acknowledges the helpful discussions with Camilo Rennó (INPE) and with the members of Geomatics Lab of the Geography Department at Humboldt-Universität zu Berlin. Research was supported by CNPq and Science Without Borders Program.

References

Aguiar, A. P. D., and Coauthors, 2012: Modeling the spatial and temporal heterogeneity of deforestation-driven carbon emissions: The INPE-EM framework applied to the Brazilian Amazon. *Global Change Biol.*, **18**, 3346–3366, doi:10.1111/j.1365-2486.2012.02782.x.

Anderson, L. O., L. Eduardo, C. De Aragão, and A. De Lima, 2005: Burn scar detection based on linear mixture model and vegetation indices using multitemporal data from MODIS/TERRA sensor in Mato Grosso State, Brazilian Amazon. *Acta Amazonica*, **35**, 445–456, doi:10.1590/S0044-59672005000400009.

Asner, G. P., E. N. Broadbent, P. J. C. Oliveira, M. Keller, D. E. Knapp, and J. N. M. Silva, 2006: Condition and fate of logged forests in the Brazilian Amazon. *Proc. Natl. Acad. Sci. USA*, **103**, 12 947–12 950, doi:10.1073/pnas.0604093103.

Barlow, J., and C. A. Peres, 2008: Fire-mediated dieback and compositional cascade in an Amazonian forest. *Philos. Trans. Roy. Soc. London*, **B363**, 1787–1794, doi:10.1098/rstb.2007.0013.

Becker, B., 2005: *Amazônia: Geopolítica na Virada do III Milênio* (*Amazonia: Geopolitics on the Verge of the Third Millennium*). 1st ed. Garamond, 180 pp.

Câmara, G., R. Souza, U. M. Freitas, J. Garrido, and F. Mitsuo, 1996: Spring: Integrating remote sensing and gis by object-oriented data modelling. *Comput. Graphics*, **20**, 395–403, doi:10.1016/0097-8493(96)00008-8.

——, D. D. M. Valeriano, and J. V. Soares, 2013: Metodologia para o cálculo da taxa anual de desmatamento na Amazônia legal. Instituto Nacional de Pesquisas Espaciais Rep., 37 pp. [Available online at http://www.obt.inpe.br/prodes/metodologia_TaxaProdes.pdf.]

Carvalho, G. O., D. Nepstad, D. McGrath, M. Diaz, M. Santilli, and A. Barros, 2002: Frontier expansion in the Amazon: Balancing development and sustainability. *Environ.: Sci. Policy Sustainable Dev.*, **44**, 34–44, doi:10.1080/00139150209605606.

Castro, E. M. R., R. Monteiro, and C. P. Castro, 2004: Atores sociais na fronteira mais avançadado pará: São Félix do Xingu e a Terra do Meio (Social agents in the state frontier: São Félix do Xingu and Terra do Meio). *Pap. NAEA*, **180**, 1–68.

Cochrane, M. A., 2003: Fire science for rainforests. *Nature*, **421**, 913–919, doi:10.1038/nature01437.

——, and M. D. Schulze, 1999: Fire as a recurrent event in tropical forests of the eastern Amazon: Effects on forest structure, biomass, and species composition. *Biotropica*, **31**, 2–16, doi:10.2307/2663955.

Congalton, R. G., and K. Green, 1999: *Assessing the Accuracy of Remotely Sensed Data: Principles and Practices*. Lewis Publications, 137 pp., doi:10.1201/9781420048568.fmatt.

EMBRAPA, 2008: Caracterização da área de estudo—Área de influência da rodovia BR-163: Zoneamento ecológico-econômico em área sob a influência da rodovia BR-163. Empresa Brasileira de Pesquisa Agropecuária, Projeto Integrado MCT-EMBRAPA, 9 pp.

Fearnside, P. M., 2005: Deforestation in Brazilian Amazonia: History, rates and consequences. *Conserv. Biol.*, **19**, 680–688, doi:10.1111/j.1523-1739.2005.00697.x.

Graça, P. M. L., 2006: Monitoramento e caracterização de áreas submetidas à exploração florestal na Amazônia por técnicas de detecção de mudanças. Instituto Nacional de Pesquisas Espaciais Rep. INPE-13644-TDI/1046, 275 pp.

Herold, M., and M. Skutsch, 2011: Monitoring, reporting and verification for national REDD + programmes: Two proposals. *Environ. Res. Lett.*, **6**, 014002, doi:10.1088/1748-9326/6/1/014002.

Hudson, W. D., and C. V. Ramm, 1987: Correct formulation of the kappa coefficient of agreement. *Photogramm. Eng. Remote Sens.*, **53**, 421–422.

IBGE, 2015: Estatística sobre Município de Novo Progresso, Pará. Instituto Brasileiro de Geografia e Estatística, accessed 16 May 2015. [Available online at http://www.cidades.ibge.gov.br/xtras/perfil.php?lang=&codmun=150503&search=para|novo-progresso.]

INPE, 2008: Monitoramento da cobertura florestal da Amazônia por satélites: Sistemas PRODES, DETER, DEGRAD e QUEIMADAS 2007-2008. Ministry of Science and Technology and INPE Rep., 47 pp. [Available online at http://www.obt.inpe.br/prodes/Relatorio_Prodes2008.pdf.]

——, 2010: Projeto TerraClass: Levantamento de informações de uso e cobertura da terra na Amazônia. Instituto Nacional de Pesquisas Espaciais, accessed 15 October 2014. [Available online at http://www.inpe.br/cra/projetos_pesquisas/terraclass.php.]

——, 2013: Projeto PRODES: Monitoramento da floresta Amazônica Brasileira por satélite (PRODES Project: Brazilian Amazon forest monitoring by satellite). Instituto Nacional de Pesquisas Espaciais, accessed 22 April 2014. [Available online at http://www.obt.inpe.br/prodes/.]

Johns, J. S., P. Barreto, and C. Uhl, 1996: Logging damage during planned and unplanned logging operations in the eastern Amazon. *For. Ecol. Manage.*, **89**, 59–77, doi:10.1016/S0378-1127(96)03869-8.

Korting, T. S., L. M. G. Fonseca, M. I. S. Escada, F. C. Silva, and M. P. Silva, 2008: GeoDMA—A novel system for spatial data mining. *IEEE Int. Conf. on Data Mining Workshops*, Pisa, Italy, IEEE, 975–978, doi:10.1109/ICDMW.2008.22.

Lambin, E. F., 1999: Monitoring forest degradation in tropical regions by remote sensing: Some methodological issues. *Global Ecol. Biogeogr.*, **8**, 191–198, doi:10.1046/j.1365-2699.1999.00123.x.

Landis, J. R., and G. G. Koch, 1977: The measurement of observer agreement for categorical data. *Biometrics*, **33**, 159–174, doi:10.2307/2529310.

Laurance, W. F., 2004: Forest-climate interactions in fragmented tropical landscapes. *Philos. Trans. Roy. Soc. London*, **B359**, 345–352, doi:10.1098/rstb.2003.1430.

Lund, H. G., 2009: What is a degraded forest? Forest Information Services Rep., 42 pp., doi:10.13140/RG.2.1.4319.7283.

Matricardi, E. A. T., D. L. Skole, M. A. Cochrane, J. Qi, and W. Chomentowski, 2005: Monitoring selective logging in tropical evergreen forests using Landsat: Multitemporal regional analyses in Mato Grosso, Brazil. *Earth Interact.*, **9**, 1–24, doi:10.1175/EI142.1.

——, ——, ——, M. Pedlowski, and W. Chomentowski, 2007: Multitemporal assessment of selective logging in the Brazilian Amazon using Landsat data. *Int. J. Remote Sens.*, **28**, 63–82, doi:10.1080/01431160600763014.

——, ——, M. A. Pedlowski, W. Chomentowski, and L. C. Fernandes, 2010: Assessment of tropical forest degradation by selective logging and fire using Landsat imagery. *Remote Sens. Environ.*, **114**, 1117–1129, doi:10.1016/j.rse.2010.01.001.

——, ——, ——, and ——, 2013: Assessment of forest disturbances by selective logging and forest fires in the Brazilian Amazon using Landsat data. *Int. J. Remote Sens.*, **34**, 1057–1086, doi:10.1080/01431161.2012.717182.

Mertens, B., and E. F. Lambin, 2000: Land-cover-change trajectories in southern Cameroon. *Ann. Assoc. Amer. Geogr.*, **90**, 467–494, doi:10.1111/0004-5608.00205.

Mertz, O., and Coauthors, 2012: The forgotten D: Challenges of addressing forest degradation in complex mosaic landscapes under REDD+. *Geogr. Tidsskr.*, **112**, 63–76, doi:10.1080/00167223.2012.709678.

Monteiro, A. L., and C. M. Souza Jr., 2012: Remote monitoring for forest management in the Brazilian Amazon. *Sustainable Forest Management: Current Research*, J. M. Garcia and J. J. D. Casero, Eds., InTech, 67–86, doi:10.5772/30126.

——, ——, and P. Barreto, 2003: Detection of logging in Amazonian transition forests using spectral mixture models. *Int. J. Remote Sens.*, **24**, 151–159, doi:10.1080/01431160305008.

Morton, D. C., R. S. Defries, J. T. Randerson, L. Giglio, W. Schroeder, and G. R. Van Der Werf, 2008: Agricultural intensification increases deforestation fire activity in Amazonia. *Global Change Biol.*, **14**, 2262–2275, doi:10.1111/j.1365-2486.2008.01652.x.

Nepstad, D., D. McGrath, A. Alencar, A. C. Barros, G. Carvalho, M. Santilli, and M. del C. Vera Diaz, 2002: Frontier governance in Amazonian. *Science*, **295**, 629–631, doi:10.1126/science.1067053.

Oravec, G. S., 1998: *Saga dos Pioneiros do Pará: Município de Novo Progresso*. 1st ed. Prefeitura Municipal de Novo Progresso, 309 pp.

Pan, Y., and Coauthors, 2011: A large and persistent carbon sink in the world's forests. *Science*, **333**, 988–993, doi:10.1126/science.1201609.

Pantoja, N., D. D. M. Valeriano, and J. V. Soares, 2011: Uso de dados da câmera HRC/CBERS-2B para estudos em áreas de exploração madeireira por corte seletivo. *Proc. 15th Simp. Brasileiro de Sensoriamento Remoto*, Instituto Nacional de Pesquisas Espaciais, Curitiba, Paraná, Brazil, 2700–2707.

Pearson, T. R. H., S. Brown, and F. M. Casarim, 2014: Carbon emissions from tropical forest degradation caused by logging. *Environ. Res. Lett.*, **9**, 034017, doi:10.1088/1748-9326/9/3/034017.

Pereira, D., D. Santos, M. Vedoveto, J. Guimarães, and A. Veríssimo, 2010: *Fatos Florestais da Amazonia 2010* (*Amazonian Forest Facts*). 1st ed. Imazon, 126 pp.

Quinlan, J. R., 1993: *C4.5: Programs for Machine Learning*. Morgan Kaufmann, 302 pp.

Ramankutty, N., H. K. Gibbs, F. Achard, R. S. Defries, J. A. Foley, and R. Houghton, 2007: Challenges to estimating carbon emissions from tropical deforestation. *Global Change Biol.*, **13**, 51–66, doi:10.1111/j.1365-2486.2006.01272.x.

Ros-Tonen, M. A. F., 2011: Changing prospects for sustainable forestry in Brazilian Amazonia: Exploring new trends. *Decentralized Development in Latin America: Experiences in Local Governance and Local Development*, P. Lindert and O. Verkoren, Eds., GeoJournal Library Series, Vol. 97, Springer, 139–153, doi:10.1007/978-90-481-3739-8_10.

Saaty, T. L., 1980: *The Analytic Hierarchy Process: Planning, Priority Setting, Resource Allocation*. 1st ed. McGraw-Hill International, 287 pp.

Sabogal, C., J. N. M. Silva, J. Zweede, R. Pereira, P. Barreto, and C. A. Guerreiro, 2000: Diretrizes técnicas para a exploração de impacto reduzido em operações florestais de terra firme na Amazônia Brasileira. CIFOR/EMBRAPA/FFT/IMAZON Rep., 24 pp.

Saito, E. A., 2011: Caracterização de trajetórias de padrões de ocupação humana na Amazonia legal por meio de mineração de dados. Instituto Nacional de Pesquisas Espaciais Rep., 160 pp.

Sasaki, N., and F. E. Putz, 2009: Critical need for new definitions of ''forest'' and ''forest degradation'' in global climate change agreements. *Conserv. Lett.*, **2**, 226–232, doi:10.1111/j.1755-263X.2009.00067.x.

Sato, L. Y., F. da Silva Ramos Viera Martins, R. Z. Cantinho, T. S. Korting, L. M. G. Fonseca, C. Almeida, and D. de Morisson Valeriano, 2011: Classificação de áreas exploradas por sistema de corte seletivo na Amazônia. *Proc. 14th Simp. Brasileiro de Sensoriamento Remoto*, Curitiba, Paraná, Brazil, Instituto Nacional de Pesquisas Espaciais, 6688–6695.

SEMA, 2015: Relatórios de Expedição de Autorização para Exploração Florestal (AUTEF). Secretaria de Estado de Meio Ambiente e Sustentabilidade, 40 pp.

Shimabukuro, Y. E., and J. A. Smith, 1991: The least-squares mixing models to generate fraction images derived from remote sensing multispectral data. *IEEE Trans. Geosci. Remote Sens.*, **29**, 16–20, doi:10.1109/36.103288.

Simula, M., 2009: Towards defining forest degradation: Comparative analysis of existing definitions. Forest Resources Assessment Working Paper, 62 pp.

Souza, C., Jr., L. Firestone, L. M. Silva, and D. Roberts, 2003: Mapping forest degradation in the eastern Amazon from SPOT 4 through spectral mixture models. *Remote Sens. Environ.*, **87**, 494–506, doi:10.1016/j.rse.2002.08.002.

——, D. Roberts, and M. Cochrane, 2005: Combining spectral and spatial information to map canopy damage from selective logging and forest fires. *Remote Sens. Environ.*, **98**, 329–343, doi:10.1016/j.rse.2005.07.013.

——, and Coauthors, 2013: Ten-year Landsat classification of deforestation and forest degradation in the Brazilian Amazon. *Remote Sens.*, **5**, 5493–5513, doi:10.3390/rs5115493.

Stone, T. A., and P. Lefebvre, 1998: Using multi-temporal satellite data to evaluate selective logging in Para, Brazil. *Int. J. Remote Sens.*, **19**, 2517–2526, doi:10.1080/014311698214604.

Tabarelli, M., J. M. C. da Silva, and C. Gascon, 2004: Forest fragmentation, synergisms and the impoverishment of neotropical forests. *Biodiversity Conserv.*, **13**, 1419–1425, doi:10.1023/B:BIOC.0000019398.36045.1b.

Thompson, I. D., M. R. Guariguata, K. Okabe, C. Bahamondez, R. Nasi, V. Heymell, and C. Sabogal, 2013: An operational framework for defining and monitoring forest degradation. *Ecol. Soc.*, **18**, 20–43.

Uhl, C., I. Celia, and G. Vieira, 1989: Ecological impacts of selective logging in the Brazilian Amazon: A case study from the Paragominas region of the state of Para. *Biotropica*, **21**, 98–106, doi:10.2307/2388700.

Valeriano, D. de M., M. I. S. Escada, G. Câmara, and M. V. Monteiro, 2012: Dimensões do desmatamento na Amazônia Brasileira. *População E Sustentabilidade Na Era Das Mudanças Ambientais Globais: Contribuições Para Uma Agenda Brasileira*, G. Martine, Ed., ABEP, 223–238.

Vasconcelos, S., P. M. Fearnside, P. M. L. de A. Graça, E. M. Nogueira, L. C. de Oliveira, and E. O. Figueiredo, 2013: Forest fires in southwestern Brazilian Amazonia: Estimates of area and potential carbon emissions. *For. Ecol. Manage.*, **291**, 199–208, doi:10.1016/j.foreco.2012.11.044.

Veríssimo, A., C. Souza Jr., S. Stone, and C. Uhl, 2008: Zoning of timber extraction in the Brazilian Amazon. *Conserv. Biol.*, **12**, 128–136, doi:10.1111/j.1523-1739.1998.96234.x.

Vieira, S., and Coauthors, 2004: Forest structure and carbon dynamics in Amazonian tropical rain forests. *Oecologia*, **140**, 468–479, doi:10.1007/s00442-004-1598-z.

Wang, C., J. Qi, and M. Cochrane, 2005: Assessment of tropical forest degradation with canopy fractional cover from Landsat ETM+ and *IKONOS* imagery. *Earth Interact.*, **9**, doi:10.1175/EI133.1.